

despite the high level of extinction. Only the end-Permian event matches the model of a “mass extinction regime” (5), arguing for a catastrophic cause consisting of a brief but major event, independent of earlier variations in diversity, with a worldwide effect and, for the most part, the nonselective demise of taxa.

References and Notes

1. D. H. Erwin, *The Great Paleozoic Crisis: Life and Death in the Permian* (Columbia Univ. Press, New York, 1993).
2. D. H. Erwin et al., *Geol. Soc. Am. Spec. Pub.* 336, 363 (2002).
3. M. J. Benton, *When Life Nearly Died: The Greatest Mass Extinction of All Time* (Thames & Hudson, London, 2003).
4. S. M. Stanley, X. Yang, *Science* 266, 1340 (1994).
5. D. Jablonski, *Science* 231, 129 (1986).
6. D. M. Raup, in *Evolutionary Paleobiology*, D. Jablonski,

- D. H. Erwin, J. H. Lipps, Eds. (Univ. of Chicago Press, Chicago, 1996), pp. 419–433.
7. A. B. Smith, C. H. Jeffery, *Nature* 392, 69 (1998).
8. D. Jablonski, *Proc. Natl. Acad. Sci. U.S.A.* 99, 8139 (2002).
9. M. Aberhan, T. K. Baumiller, *Geology* 31, 1077 (2003).
10. M. Foote, *Paleobiology* 19, 185 (1993).
11. K. Roy, M. Foote, *Trends Ecol. Evol.* 12, 277 (1997).
12. C. N. Ciampaglio, M. Kemp, D. W. McShea, *Paleobiology* 27, 695 (2001).
13. W. B. Saunders, D. M. Work, S. V. Nikolaeva, *Paleobiology* 30, 19 (2004).
14. J. Kullmann, D. Korn, *GONIAT Version 3.1, Paleozoic Ammonoid Database System* (Univ. of Tübingen, 2002).
15. T. B. Leonova, *Paleontol. J.* 36 (suppl. 1) (2002).
16. Z. Zhou et al., *Permophiles* 29, 195 (1996).
17. S. E. Peters, M. Foote, *Paleobiology* 27, 583 (2001).
18. S. E. Peters, M. Foote, *Nature* 416, 420 (2002).
19. M. A. Wills, in *Fossils, Phylogeny, and Form—An Analytical Approach*, J. M. Adrain et al., Eds. (Kluwer Academic/Plenum, New York, 2001), pp. 55–144.

20. See supporting data on Science Online.
21. B. F. Glenister, W. M. Furnish, in *The Ammonoidea*, M. R. House, J. R. Senior, Eds. (Academic Press, London, 1981), pp. 49–64.
22. C. N. Ciampaglio, *Evol. Dev.* 6, 260 (2004).
23. W. B. Saunders, D. M. Work, S. V. Nikolaeva, *Science* 286, 760 (1999).
24. We thank D. Lazarus, D. Unwin, G. J. Eble, and W. Kiessling for discussions. Supported by a post-doctoral fellowship of the Alexander von Humboldt Foundation (L.V.) and by the Deutsche Forschungsgemeinschaft (D.K.). This is Paleobiology Database publication number 28.

Supporting Online Material

www.sciencemag.org/cgi/content/full/306/5694/264/DC1
 Materials and Methods
 Figs. S1 to S5
 Table S1
 References

29 June 2004; accepted 25 August 2004

The Scaling of Animal Space Use

Walter Jetz,^{1,2*}† Chris Carbone,³ Jenny Fulford,³ James H. Brown²

Space used by animals increases with increasing body size. Energy requirements alone can explain how population density decreases, but not the steep rate at which home range area increases. We present a general mechanistic model that predicts the frequency of interaction, spatial overlap, and loss of resources to neighbors. Extensive empirical evidence supports the model, demonstrating that spatial constraints on defense cause exclusivity of home range use to decrease with increasing body size. In large mammals, over 90% of available resources may be lost to neighbors. Our model offers a general framework to understand animal space use and sociality.

Space use in animals is strongly tied to body size and has been a focal point of ecological research (1–7). This research has led to the formulation of scaling rules—power law relations between body size and animal area use—in two separate lines of research: population density and home range size. Here we develop a simple model for the use of space by animals that incorporates energy requirements and interactions with neighbors to unify these approaches.

We assume that energy and material resource requirements are determined by the whole-organism field metabolic rate B (in units of kJ/day or watts), which has been shown to scale as

$$B = B_0 M^{3/4} \quad (1)$$

¹Department of Ecology and Evolutionary Biology, Princeton University, Princeton, NJ 08544–1003, USA. ²Department of Biology, University of New Mexico, Albuquerque, NM 87131, USA. ³Institute of Zoology, Zoological Society of London, Regent’s Park, London, NW1 4RY, UK.

*To whom correspondence should be addressed. E-mail: wjetz@princeton.edu

†Address as of December 2004: Division of Biological Sciences, University of California, San Diego, La Jolla, CA 92093, USA.

B_0 is a normalization constant that also incorporates the diet-specific assimilation efficiency, which determines the proportion of ingested energy available for activity. Let H be the home range area in km² and R the species-specific rate of supply of usable resources available in H , in units of W/km². However, intrusions from foraging conspecific neighbors into a portion of the home range may decrease the proportion of R available to the home range owner (8). This resource depletion can be put into a spatial context by thinking in terms of a portion of the home range that is used exclusively only by the owner, H_o , and a portion that overlaps with neighbors and whose resources are harvested only by intruders. We use α to designate the proportion of the resource supply rate across a home range that is harvested exclusively by the owner: $\alpha = H_o R / HR$. This can be simplified to

$$\alpha = H_o / H \quad (2)$$

Accordingly, the proportion of resource supply rate taken by the neighbors, or home range overlap, is $1 - \alpha$.

It follows that if an individual uses an area just sufficient to meet its metabolic

requirements, it requires a home range of area

$$H = B / \alpha R = B_0 R^{-1} \alpha^{-1} M^{3/4} \quad (3)$$

Population density, N , can be used to empirically quantify α . Its reciprocal, N^{-1} indicates the average area per individual and is equivalent to H_o , and thus from Eq. 2 it follows that

$$\alpha = N^{-1} / H \quad (4)$$

Finally, the scaling of N^{-1} is identical to that of H , without the effect of neighbors on scaling and normalization constant

$$N^{-1} = B / R = B_0 R^{-1} M^{3/4} \quad (5)$$

These equations can serve to illustrate three potential scenarios for the scaling of home range size that are dependent on the examination of the two key parameters, R and α . (i) Both α and R are body size-invariant ($R \propto M^0$ and $\alpha \propto M^0$). This is the hypothesis initially proposed by McNab (1). It predicts that home range size should scale as $M^{3/4}$ ($H \propto M^{3/4}$), but it was not supported by subsequent analyses indicating home range scaling close to 1 (9–12). (ii) R decreases with body size approximately to the quarter power, whereas α is body size-invariant ($R \propto M^{-1/4}$ and $\alpha \propto M^0$). This predicts the observed $H \propto M^1$. This idea was originally proposed by Harestadt and Bunnell (13) and recently refined by Haskell et al. (14), who modeled the potential interaction between the fractal distribution of resources and foraging mode. This scenario predicts that larger species require larger home ranges than the scaling of their energy needs alone would suggest, because of their lower encounter rates with food items. Because R affects the scaling of both N^{-1} and H equally (compare Eqs. 3 and 5), their scaling lines should have no distinct intersection. (iii) Resource supply rate R does not scale with body size, but proportional access by the home range owner, α , scales approximately to the negative one-

quarter power ($R \propto M^0$ and $\alpha \propto M^{-1/4}$), leading to the observed $H \propto M^1$ and an intersection of the scaling lines. A potential role of home range overlap with neighbors has been pointed out previously (7, 15, 16), but an understanding of the scaling remains little developed. Here we develop a new theory that quantifies the effect of neighbors, α , and provide an empirical test for all core scenarios for the scaling of animal space use.

Larger home ranges are more difficult to defend from intrusion. This idea is supported by field observations (8), but its conceptual basis can be seen by considering the task of defending an increasing area (fig. S1). From Eq. 3, it follows that the minimum area of a home range in the absence of competition scales as $M^{3/4}$. It has been found empirically that the day range, or the average distance traveled in 1 day, scales as $M^{1/4}$ (16–18). Hypothetically, this is equivalent to a mouse traveling 110 m in a 70-m-diameter home range, versus an elephant traveling 2 km in a 6-km-diameter home range. Clearly, the larger animal faces a more formidable task of detecting and minimizing overlap with intruders.

The magnitude of this task can be modeled quantitatively by using the equation from physics for collisions among gas particles to predict the frequency of interactions between owners and intruders (19–21). In two-dimensional space, the frequency of interactions f among individuals is

$$f = \frac{4}{\pi} N D d \quad (6)$$

where N is the population density (in individuals per km^2), D is the average speed (the day range in km traveled per day), and d is the average neighbor interaction distance (in km). We use the above well-established scaling relations to characterize how density and speed of movement vary with body size: $N \propto M^{-3/4}$ (5) and $D \propto M^{1/4}$ (7, 16–18). Less is known about the scaling of interaction distance, which is likely to vary with communication system and habitat structure. Limited sources indicate a scaling of detection distance between M^0 and $M^{1/2}$ (17, 22, 23), and here we attempt a first test of its effect using the midpoint, $d \propto M^{1/4}$, the scaling of a typical biological distance (7, 24, 25).

We assume that interactions with conspecific neighbors lead to temporary reinforcement of exclusive home range use and hence to reduced resource extraction by home range intruders (2). All else being equal, neighbors that encounter each other more frequently should be able to maintain more fixed home range boundaries and thus get by with relatively smaller home ranges, because the resources are used more exclusively. Quantitatively, we assume that the proportion of the total resources or proportional home range area that is exclusive to a home range owner,

α , is proportional to the neighbor interaction frequency, so $\alpha \propto f$. Substituting the assumed allometric scalings of population density, day range, and interaction distance into Eq. 4 gives the predicted scaling of α

$$\alpha \propto f \propto M^{-3/4} M^{1/4} M^{1/4} \propto M^{-1/4} \quad (7)$$

The assumption of random movement in Eq. 6 can be relaxed to allow a wide variety of movement patterns without altering Eq. 7; the critical feature is that the way owner and intruder move with respect to each other is independent of body size. We now modify Eq. 3 to model home range area, incorporating the fraction of the total home range whose resources are used by the neighbor. Following scenario (iii) and assuming body size invariance of resource supply rate R this leads to

$$H = B/\alpha R = B_0 R^{-1} M^{1/4} M^{3/4} = B_0 R^{-1} M^1 \quad (8)$$

The above equations provide a simple general model for how animals use space and interact with neighbors. This model makes a number of predictions that can be tested empirically. We use two extensive compilations on home range size and population density in mammals (11, 26) to test the model predictions. In order to account for the effect of grouping in the context of our model, we perform our analyses with home range size per individual, $H = (\text{observed home range}/\text{social unit size})$, as a response (27).

A log-log plot of H as a function of M has a slope of 1.07, which is not statistically distinguishable from the value of 1 estimated in Eq. 8 (Fig. 1 and Table 1) but is significantly higher than 0.75, which rejects body size invariance of R and α predicted by scenario (i) (1). A log-log plot of N^{-1} , the reciprocal of population density, as a function

of M has a slope of 0.76 (Fig. 1 and Table 1), which is almost identical to the value of 3/4 predicted in Eq. 5, given body size invariance of R [see also (5, 28–30)]. Across trophic groups, the slopes vary from 0.73 to 0.86 but are never significantly different from 0.75 (t tests, $P > 0.1$ in all cases). This supports the assumption of scenario (iii) that resource supply rate R is body size-independent ($R \propto M^{-0.02}$ to $M^{0.11}$ across trophic levels) and rejects the supply rate-based scenario (ii) for the scaling of home range size (13, 14). The intercepts of the relations in Figs. 1 and 2 at $M = 1$ kg indicate the ratio between energy expenditure and energy supply rate (B_0/R) as a function of body size. Given empirical estimates of mammalian field metabolic rates and assimilation efficiencies, we can estimate how the different area needs point to the highly different resource supply rate experienced across trophic levels. We find that the energy supply rate R is approximately 2188 W km^{-2} in herbivores, 408 W km^{-2} in omnivores, and 32 W km^{-2} in carnivores, independent of body size.

Following Eq. 4, the difference in scaling exponents of H and N^{-1} , or their slopes on the log-log plot with body size (Fig. 1), indicates the value of α , proportional home range exclusivity. We find that α is statistically different from zero in all trophic groups and ranges from 0.26 to 0.39, without any consistent effect of diet (Table 1). These values are not different from those predicted by Eqs. 7 and 8 (t tests, $P > 0.1$ in all cases). Together with the body size independence of R , these results support scenario (iii), the proposed scaling of neighbor interaction, as a general mechanism explaining the scaling of animal space use in the presence of neighbors.

We can further estimate the home range exclusivity at a given body size by synthesizing

Fig. 1. The body size dependence of individual area use and overlap in mammals. (A) Individual home range size H , corrected for grouping. (B) Per-individual area use or reciprocal density, N^{-1} . (C) The above scaling relations of H (solid line) and N^{-1} (dashed line) plotted together for comparison. (D) The resulting scaling of α (in percent); that is, the percentage of resources exclusively taken by the home range owner or percent of home range overlap is given as $1-\alpha$ as percentage). Data points are species; thick lines are least-squares fits; dotted lines are their 95% confidence intervals. For detailed regression results, see Table 1.

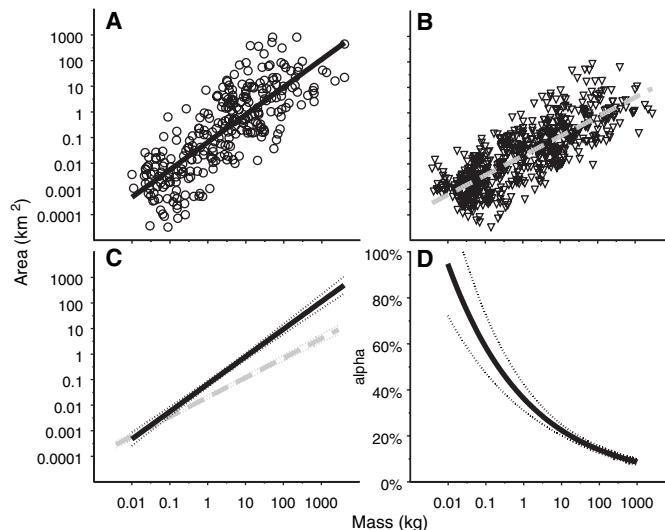


Table 1. Observed scaling relations of per-individual area use in mammals. Data are obtained from two measures: the inverse of population density (N^{-1}) and individual home range size (H , corrected for group size). These data are also analyzed by trophic level, herbivores (Herb), omnivores (Omn), and carnivores (Carn). The slope analysis gives the individual scaling exponents m

and the scaling exponents for α , proportional home range exclusivity, which are given as $\alpha = m(N^{-1}) - m(H)$, where m refers to the calculated scaling exponents. Numbers in brackets are the 95% confidence intervals. The r^2 values are based on log-transformed data. n indicates sample size (number of species).

		n	Cross over		Intercept		Slope		Model	
			M (kg) at $N^{-1} = H$	Area (ha) at $M = 1$	m	$\alpha \propto M^x$	F	r^2		
All	H	274	0.022 (0.215)	6.69 (1.68)	1.07 (0.10)	-0.31 (0.11)	464.3	0.63		
	N^{-1}	563							2.06 (0.28)	0.76 (0.05)
Herb	H	158	0.064 (0.260)	1.01 (0.01)	0.76 (0.05)	-0.26 (0.11)	948.7	0.74		
	N^{-1}	327							2.05 (0.03)	1.02 (0.09)
Omn	H	44	0.022 (0.187)	15.87 (1.30)	1.12 (0.15)	-0.39 (0.18)	208.5	0.83		
	N^{-1}	176							3.62 (0.09)	0.73 (0.09)
Carn	H	70	0.299 (0.596)	52.07 (10.87)	1.20 (0.19)	-0.34 (0.28)	157.8	0.70		
	N^{-1}	38							34.43 (4.03)	0.86 (0.20)

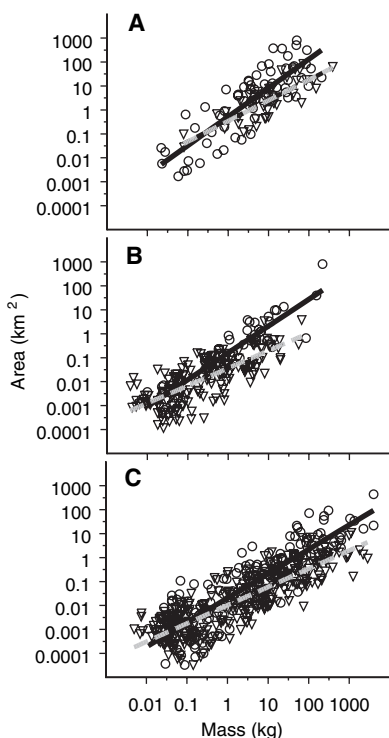


Fig. 2. The scaling across trophic levels of per-individual area (N^{-1} , triangles, dashed line) and individual home range size (H , circles, solid line). (A) Carnivores. (B) Omnivores. (C) Herbivores. Lines are least-squares fits. For detailed regression results, see Table 1.

the data for N and H . In a fully filled landscape, we expect individual home range size to be at least equal to the area per individual, $H \geq N^{-1}$. Because the model predicts increasing overlap in home ranges with increasing size, it follows that log-log plots of H and N^{-1} as function of M should be nearly coincident for the smallest mammals but diverge with increasing body mass. This is exactly what is observed (Figs. 1 and 2). The regression equations for all mammals suggest that although neighbor effects are negligible at the smallest body sizes, already at 1 kg only 31% of home range or resource supply rate is

obtained by the owner, and just 7% at 100 kg (Fig. 1). These surprising results are robust to a more restrictive analysis using only species with data on both H and N^{-1} (table S1), and they highlight the so-far-underappreciated magnitude of neighbor effects.

Our finding of extensive home range overlap at all but the smallest body sizes falsifies key assumptions of hypotheses on the scaling of animal space use that assume exclusive access to resources (12) or, additionally, a body size dependence of resource supply rate (13, 14). Population estimates of large-bodied species are as much as an order of magnitude higher than suggested by home range size. This finding is counter to the idea that increased census areas and the inclusion of unsuitable habitat have led to underestimates of population densities for large-bodied animals [(31), but see (32)]. Indeed, the high degree of home range overlap in large mammals suggests that population density rather than home range size is the better measure to use in quantifying individual area needs for conservation purposes.

Our findings resolve a long-standing conflict resulting from two divergent approaches to studying the use of space in animals, based on home range size and population density. Our approach provides a simple and powerful framework for understanding how animal space use reflects the constraints of both harvesting resources and detecting and responding to intruders. It has important applications in other behavioral ecological phenomena, such as group living, mate finding, disease transmission, and predator-prey encounters. Our results show how mechanistic models based on first principles of physics, ecological energetics, and behavioral ecology can make testable predictions and enhance our understanding of macroecological patterns.

References and Notes

1. B. K. McNab, *Am. Nat.* **97**, 133 (1963).
2. L. Witting, *J. Theor. Biol.* **177**, 129 (1995).
3. T. M. Blackburn, K. J. Gaston, *J. Anim. Ecol.* **66**, 233 (1997).
4. R. H. Peters, K. Wassenberg, *Oecologia* **60**, 89 (1983).
5. J. Damuth, *Nature* **290**, 699 (1981).

6. M. Silva, M. Brimacombe, J. A. Downing, *Global Ecol. Biogeogr.* **10**, 469 (2001).
7. W. A. Calder, *Size, Function and Life History* (Harvard Univ. Press, Cambridge, MA, 1984).
8. J. W. A. Grant, C. A. Chapman, K. S. Richardson, *Behav. Ecol. Sociobiol.* **31**, 149 (1992).
9. G. Mace, P. H. Harvey, *Am. Nat.* **121**, 120 (1983).
10. T. W. Schoener, *Ecology* **49**, 123 (1968).
11. D. A. Kelt, D. H. Van Vuren, *Am. Nat.* **157**, 637 (2001).
12. S. L. Lindstedt, B. J. Miller, S. W. Buskirk, *Ecology* **67**, 413 (1986).
13. A. S. Harestad, F. L. Bunnell, *Ecology* **60**, 389 (1979).
14. J. P. Haskell, M. E. Ritchie, H. Olff, *Nature* **418**, 527 (2002).
15. J. Damuth, *Biol. J. Linn. Soc.* **15**, 185 (1981).
16. R. K. Swihart, N. A. Slade, B. J. Bergstrom, *Ecology* **69**, 393 (1988).
17. T. Garland, *Am. Nat.* **121**, 571 (1983).
18. C. Carbone, G. Cowlshaw, N. J. B. Isaac, J. M. Rowcliffe, *Am. Nat.*, in press.
19. P. M. Water, *Am. Nat.* **110**, 911 (1976).
20. A. Okubo, *Diffusion and Ecological Problems: Mathematical Models; Biomathematics* (Springer-Verlag, Berlin, 1980).
21. L. Barrett, C. B. Lowen, *Funct. Ecol.* **12**, 857 (1998).
22. R. A. Kiltie, *Funct. Ecol.* **14**, 226 (2000).
23. K. Kirschfield, in *Neural Principles in Vision*, F. Zettler, R. Weiler, Eds. (Springer, Berlin, 1976), pp. 354–370.
24. V. M. Savage, J. F. Gillooly, J. H. Brown, G. B. West, E. L. Charnov, *Funct. Ecol.* **18**, 257 (2004).
25. R. H. Peters, *The Ecological Implications of Body Size* (Cambridge Univ. Press, Cambridge, 1983).
26. J. Damuth, *Biol. J. Linn. Soc.* **31**, 193 (1987).
27. Materials and methods are available as supporting material on Science Online.
28. C. Carbone, J. L. Gittleman, *Science* **295**, 2273 (2002).
29. P. A. Marquet, *Science* **295**, 2229 (2002).
30. S. K. M. Ernest *et al.*, *Ecol. Lett.* **6**, 990 (2003).
31. T. M. Blackburn, K. J. Gaston, *Oikos* **75**, 303 (1996).
32. C. N. Johnson, *Oikos* **85**, 565 (1999).
33. We are indebted to D. A. Kelt and D. H. Van Vuren for granting us access to their compilation of home range data and to J. Damuth for making his population density data publicly available. We thank A. P. Allen, E. L. Charnov, S. K. M. Ernest, A. P. Dobson, A. B. Herman, D. Rubenstein, R. P. Freckleton, J. L. Gittleman, P. H. Harvey, J. M. C. Hutchinson, N. J. B. Isaac, M. V. McPhee, H. Olff, J. M. Rowcliffe, V. Savage, D. Storch, J. S. Weitz, and E. P. White for inspiring discussions and helpful feedback on the manuscript. W.J. gratefully acknowledges support from the German Academic Exchange Service (DAAD) and the German Research Foundation (Deutsche Forschungsgemeinschaft).

Supporting Online Material

www.sciencemag.org/cgi/content/full/306/5694/266/DC1
 Materials and Methods
 Fig. S1
 Table S1
 References

29 June 2004; accepted 12 August 2004

Keeping an Eye on the Neighbors

Steven Buskirk

For decades ecologists have sought to understand the principles underlying how mammals optimize their space requirements. It is intuitive that mammals need home ranges: areas they routinely traverse that are large enough to meet their energy needs, but small enough to be protected from intrusions by same-species neighbors that occupy adjacent home ranges. Early attempts to understand the relation between body mass and home-range area suggested that home-range area increases at the same rate as metabolism (1). As metabolic rate is proportional to body mass raised to the $3/4$ power, then home-range size should also have the same proportion to body mass (2). However, abundant data on the home ranges of mammals, primarily derived from wildlife telemetry studies, suggest that this is not the case. Indeed, the home-range area increases at a higher rate than metabolic rate and, in fact, scales almost linearly with body mass (3, 4). Yet parallel evidence from mammalian population density studies is consistent with a metabolic explanation of individual spatial requirements in that the reciprocal of population density (area per animal) appears to scale to the $3/4$ power of body mass (5). As large mammals have home ranges bigger than would be predicted from their energetic needs, this implies a maintenance cost that goes beyond the acquisition of essential resources. On page 266 of this issue, Jetz and co-workers (6) coalesce all of these findings by deriving a general model of mammalian spatial requirements that incorporates body mass, energy requirements, home-range size and, crucially, interactions with same-species neighbors. Cleverly, the authors use an equation from physics for collisions among gas particles to predict the frequency of interactions between home-range owners and intrusive neighbors. They show that large mammals require a home range that is larger than predicted by resource needs because they share resources with their neighbors to a greater extent than do small mammals (see the figure). This forced sharing is the result of body size-dependent processes, such as whether the mammal is able to traverse its home range often enough to exclude its neighbors.

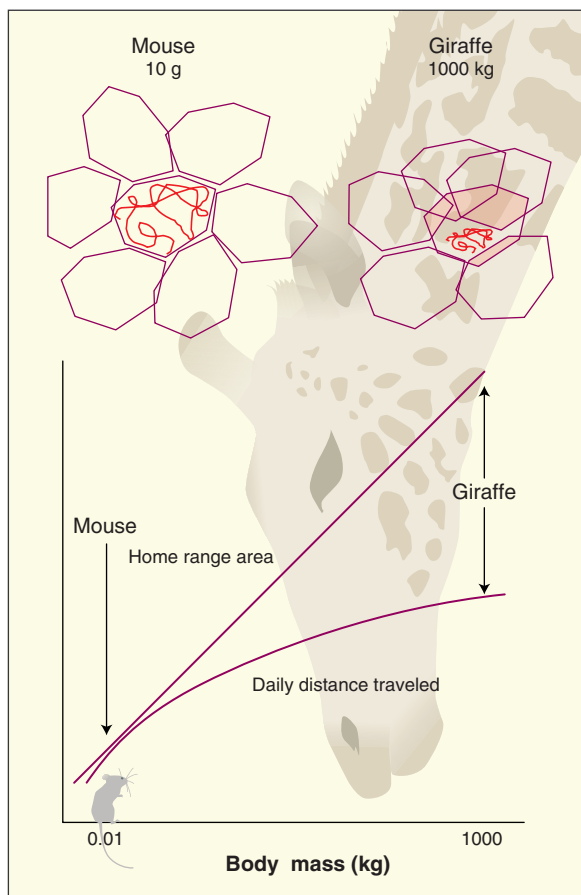
Jetz *et al.*'s general approach falls within the realm of allometric macroecology,

which attempts to explain biological differences among species by examining patterns over a wide range of body sizes (7). For terrestrial mammals, this range is represented by the six orders of magnitude that separate the body masses of shrews and elephants. Metabolic rate, the most fundamental of physiological attributes, was shown by Kleiber (1) to be proportional to the $3/4$ power of body mass in mammals across an entire range of body sizes, rather than the $2/3$ power predicted by a

simple surface area to volume relation. Recently the $3/4$ exponent was derived from first principles by West and co-workers (8). Home range is one of the most integrative of ecological variables, and so several confounding factors must be taken into account when calculating home-range size. For example, carnivores have larger home ranges than do herbivores of the same size, so that data sets in which trophic level and body size are correlated produce biased scaling exponents. Species living at high latitudes and altitudes have disproportionately larger home ranges, so correlations between body size or trophic level and latitude must be considered. In addition, the fact that sociality varies with body size in mammals needs to be taken into account. Large mammals, such as moose, giraffes,

elephants, and bison, tend to live in groups; shrews and mice are mostly solitary. Thus, for large mammals, a group of animals needs to be considered as the "occupant" of the home range.

The most problematic factor, however, is the allometric dependence of home-range maintenance behaviors, including interactions by occupants—individuals or groups—with same-species neighbors. These interactions temporarily deter neighbors from forays into the occupant's home range, so that home-range overlap is reduced. The more frequently an occupant patrols its home range, the better the opportunity to maintain the exclusivity of the home range, and limit home-range size to the energetic optimum. The ability to traverse the home range and deter visits by neighbors decreases rapidly with increasing body size: Daily distance traveled scales with a body-size exponent $1/4$ of that for home-range area. So, large mammals are unable to cover the home range often enough to exclude their neighbors (see the figure). Sharing parts of the home range with neighbors means sharing resources, necessitating a larger home range to ensure that energy requirements are met. It might seem that home-range boundaries would completely break down at



The mathematics of personal space. The ability of mammals to traverse their home ranges (polygons) and exclude same-species neighbors scales with body size. Small mammals, such as the mouse, cover their home ranges (red path) in a short time, interact with neighbors, and maintain exclusive home ranges. Large mammals, such as the giraffe, take longer to cover their home ranges, so that frequent interactions with neighbors is impossible. As a result, large mammals are unable to maintain an exclusive home range and must share parts of the home range (pink shaded area) and resources with intrusive neighbors. Such forced sharing means that the home ranges of larger mammals need to be bigger than that predicted from their resource requirements.

The author is in the Department of Zoology and Physiology, University of Wyoming, Laramie, WY 82071, USA. E-mail: marten@uwyo.edu

some body size, but such a shift to nomadism has not been observed.

An ingenious aspect of the approach taken by Jetz *et al.* is their adaptation of a model of molecular collisions in gas to the allometry of encounters between home-range occupants and their neighbors. In the adapted model, frequency of interaction is a function of population density, speed of movement, and the distance at which two animals may be said to have “collided”—that is, the interaction distance. They evaluated each of these factors with regard to its potential relation to body size. In the case of the interaction distance, evidence is accumulating that mammals detect and communicate with each other at distances that scale with a body-mass exponent of less than 1 (9). Previous workers (4) have not considered the scaling of interaction distance, but Jetz and co-workers assume

that a body-mass exponent of $1/4$ —typical for ecological distances—might approximate this relation. Using this value, home-range size should be proportional to body mass raised to the power of 1, which is very close to the observed values.

Jetz and co-workers have made the most recent contribution to the emerging field of metabolic ecology (7), which aims to explain population, landscape, and ecosystem patterns in terms of basic mathematical and physical principles. They also have resolved long-standing confusion about how to scale the spatial needs of mobile animals. Their elegant model will guide future exploration and hypothesis testing in this area. An important remaining task is to more accurately measure the scaling of neighbor detection—that is, the maximum distance apart that mammals of different sizes can be and yet still detect their same-

species neighbors. Happily, the Jetz study is not without implications for conservation. Those planning viable mammalian populations should attend more closely to the scaling of population density than to the scaling of home-range size. Concentrating on the scaling of home-range size, a common approach, drastically overestimates the spatial requirements for populations. This unnecessarily constrains planning for viable mammalian populations, especially of the largest mammals.

References

1. M. Kleiber, *The Fire of Life* (Wiley, New York, 1961).
2. B. K. McNab, *Am. Nat.* **97**, 133 (1963).
3. A. S. Harestad, F. L. Bunnell, *Ecology* **60**, 389 (1979).
4. S. L. Lindstedt *et al.*, *Ecology* **67**, 413 (1986).
5. J. Damuth, *Biol. J. Linn. Soc.* **31**, 193 (1987).
6. W. Jetz *et al.*, *Science* **306**, 266 (2004).
7. J. H. Brown *et al.*, *Ecology* **85**, 1771 (2004).
8. G. B. West *et al.*, *Science* **276**, 122 (1997).
9. R. A. Kiltie, *Funct. Ecol.* **14**, 226 (2000).

DEVELOPMENT

ES Cells to the Rescue

Kenneth R. Chien, Alessandra Moretti and Karl-Ludwig Laugwitz

Unlocking the therapeutic potential of embryonic stem (ES) cells has remained a tantalizing but elusive goal. In this new era of “regenerative medicine,” the central experimental game plan has been predicated on driving the differentiation of ES cells along specific cell lineages (for example, neural, cardiac, endocrine), expansion and purification of the cell type of interest, and in vivo repopulation of damaged or degenerating organs by ES cell-derived differentiated cells. However, there are numerous hurdles to using ES cells as therapeutic tools. These include the need for reliable ES cell differentiation protocols for different cell lineages, purification techniques for the differentiated progeny, as well as ways to circumvent the immunological rejection of transplanted cells. Given the complexity of these multiple steps, it is not surprising that there are few clear examples of in vivo ES cell therapy for treating disease-related phenotypes. On page 247 of this issue, an exciting new study by Fraidenraich and co-workers (1) expands the potential therapeutic repertoire of ES cells (2). These investigators provide direct evidence that ES cells can rescue otherwise lethal cardiac defects in mouse embryos. Intriguingly, the rescue effect is not subject to the differentiation of ES cells into the cardiac cell lineages that are normally associated with heart regeneration. Rather, the

therapeutic effect of the transplanted ES cells depends on their secretion of defined factors that act either locally within the embryonic heart, or at a distance via the maternal circulation, to trigger fetal myocyte proliferation in utero.

In the new study, Fraidenraich and colleagues (1) report a prominent cardiac phenotype in mouse embryos that harbor a double or triple deletion (knockout) of the *Id1*, *Id2*, and *Id3* genes. The proteins encoded by these genes are transcriptional regulators that affect the differentiation of multiple cell types. The mutant *Id* embryos die at mid-gestation due to a marked thinning of the myocardial wall. This cardiac defect has been found in a number of mutant mouse embryos, including those lacking RXR- α (3–5), gp 130 (6), or other signaling proteins (7). In all of these cases, the signals that link these proteins to thinning of the myocardial wall appear to arise from noncardiac muscle cells, and many of these proteins are not expressed in myocardial cells. Previously, approaches such as chimera rescue (8) and cardiac lineage-restricted knockout of target genes (9, 10) indicated that a non-cell autonomous pathway causes the onset of “thin myocardial wall” syndrome (that is, the defect does not involve myocardial cells). Indeed, several of these studies implicate another section of heart tissue called the epicardium in myocardial wall thinning (see the figure).

In the new work, Fraidenraich and co-workers report that their mutant *Id* mouse

embryos display a loss of myocardial proliferative capacity, and marked dysregulation of a panel of cardiac genes revealed by gene profiling (1). The *Id* gene family is not expressed in the myocardium, but is expressed in the epicardium. The investigators note that conditioned medium from primary cultures of epicardial cells derived from wild-type embryos rescue the proliferative defect in cultured heart cells from the mutant mice. In contrast, conditioned medium derived from the *Id* mutant embryos had no activity, showing that the rescue effect is specific. Their chimeric embryo studies also support a non-cell autonomous pathway that links the loss of *Id* signals from outside the myocardium with the cardiac defect. The authors found that injection of mutant blastocyst embryos with as few as 15 wild-type ES cells rescued a subset of the cardiac defects and prevented death of the embryos. Surprisingly, the authors go on to show that the intraperitoneal injection of ES cells into female mice prior to conception also partially rescued the cardiac phenotype and prevented embryonic lethality (see the figure). A brain vascular defect that causes brain hemorrhaging also was rescued, suggesting that the secreted rescue factors act from a distance on at least two distinct target tissues of the embryo. By using ES cells with reduced *Id* gene expression, the authors show that the rescue effect is specific for *Id*-related pathways. Through microarray analyses, they went on to pinpoint two factors that exhibit partial rescue of the cardiac defect: Wnt5a and IGF-1 (insulin-like growth factor 1). Wnt5a is a local paracrine factor produced in the epicardium of the fetal heart that directly promotes the proliferation of neighboring embryonic cardiac

The authors are in the Institute of Molecular Medicine, University of California San Diego, La Jolla, CA 92037, USA. E-mail: kchien@ucsd.edu